

Activation-energy spectrum and structural relaxation dynamics of amorphous silicon

Jung H. Shin and Harry A. Atwater

Thomas J. Watson Laboratory of Applied Physics, California Institute of Technology, Pasadena, California 91125

(Received 10 August 1992; revised manuscript received 5 March 1993)

The structural relaxation dynamics in pure (unhydrogenated) amorphous silicon (*a*-Si) following ion-irradiation-induced defect injection is investigated by measuring the changes in electrical conductivity. It is found that the conductivity of *a*-Si decreases over three orders of magnitude upon relaxation by defect annihilation. Subsequent ion irradiation reverses the conductivity changes, confirming that the observed conductivity change is solely due to structural relaxation. Through a combined analysis of both *in situ* and *ex situ* measurements of dynamics of change in conductivity upon structural relaxation, the density of relaxation states with activation energy Q associated with localized electron states near the Fermi level is measured. It is found to be a continuous, monotonically decreasing function extending from $Q < 0.9$ eV to $Q > 2.5$ eV, and *in situ* measurement of conductivity suggests a lower limit of $Q < 0.23$ eV. Knowledge of this quantity in turn enables a quantitative estimate of the activation energy spectrum for structural relaxation of *a*-Si. Results are compared with previous investigations of structural relaxation and solid-phase epitaxy of *a*-Si, and the relevance of defect injection and structural relaxation in *a*-Si to irradiation-enhanced nucleation of crystal silicon is discussed.

I. INTRODUCTION

Structural relaxation refers to the slow atomic transport processes that occur in amorphous solids, which lead to a reduction in free energy while retaining the amorphous phase. Much work has been done in studying structural relaxation and its counterpart, structural unrelaxation, in amorphous silicon. Pure (i.e., unhydrogenated) amorphous silicon (*a*-Si) is a model system for study of covalently bonded amorphous solids characterized as continuous random networks. It is now well established that many properties of *a*-Si (e.g., refractive index,¹ spin density,¹ viscosity,² enthalpy,^{3,4} vibrational properties,^{5,6} diffusivity,^{7,8} and shear viscosity⁹) are dependent upon the extent of structural relaxation.

As is true of other amorphous solids, the structural relaxation kinetics of *a*-Si is not characterized by a single activation energy. For instance, Roorda, *et al.*¹⁰ have shown, using differential isothermal calorimetry measurements, that defects with many different activation energies contribute to relaxation. However, due to the lack of an explicit understanding of the enthalpy released upon defect annihilation in *a*-Si, no quantitative analysis of the activation-energy spectrum has been attempted. On the other hand, theories for electrical conductivity of *a*-Si are well developed and supported by experimental data. It is also well established that the electrical conductivity of *a*-Si is sensitively dependent on the degree of relaxation.¹¹ Hence, conductivity measurements of *a*-Si allow the study of defects which directly affect the conductivity,¹² as has been done in metallic glasses.¹³ By combining existing models for structural relaxation of amorphous solids and for electrical conductivity of *a*-Si, we were able to quantitatively analyze the relaxation dynamics and activation-energy spectrum associated with structural defects in *a*-Si which affect conductivity. Recently, Coffa

and Poate¹⁴ have shown that passivating ion-irradiated *a*-Si by hydrogen has the same effect on diffusion of transition metals as structural relaxation does. Hydrogen is well known to passivate electrically active defects in *a*-Si, and decrease the electrical conductivity by reducing the number of localized electronic states in the energy gap.¹⁵ Thus, it is reasonable to suppose that the results we obtained for electrically active structural defects are indeed a good indication of the overall structural relaxation dynamics of *a*-Si. We will also comment on the implication of our result for the relationship between structural relaxation and the rate of solid-phase epitaxy (SPE) of crystal silicon (*c*-Si) into *a*-Si, and on irradiation-enhanced nucleation of crystal silicon in an *a*-Si matrix.

II. EXPERIMENTAL PROCEDURE

Pure amorphous silicon films 4500 Å thick were grown on thermally oxidized Si substrates by ultrahigh vacuum electron-beam deposition. The oxide layer was 1.1 μm thick. Prior to loading into the deposition system, substrates were cleaned by immersion in a 5:1:1 solution of H₂O:H₂O₂:NH₄OH at 80°C, followed by a rinse in ultrahigh purity deionized H₂O. Prior to deposition, the substrates were sputter cleaned by 100 eV Ar-ion bombardment, and the silicon evaporation source material was outgassed. The system base pressure is in the 10⁻¹⁰ Torr range, but the pressure rose to 5 × 10⁻⁸ Torr during deposition. The dominant constituent of this pressure rise was due to the partial pressure of hydrogen. The substrate temperature during deposition was ~373 K, and the deposition rate was 2 Å sec⁻¹. Immediately following deposition, and prior to exposure to air, the films were heated at 620 K for 1 h to densify *a*-Si and to remove microscopic voids which otherwise might lead to substantial trapping of oxygen and water vapor.¹⁶ Fol-

lowing deposition, *a*-Si thin-film resistors on silicon dioxide were defined by lithography and wet chemical etching. The photolithographic steps necessary for thin-film resistor and contact formation required samples to be annealed briefly at 473 K. Aluminum contacts were evaporated for samples subject to temperatures less than 573 K during conductivity measurements. Samples subject to temperatures higher than 573 K during conductivity measurements employed sputter-deposited Ag contacts with amorphous Ti/Si/N diffusion barriers between the Ag contacts and *a*-Si. Amorphous Ti/Si/N diffusion barriers are known to be effective up to 900 K with crystallization temperatures in excess of 1273 K.¹⁷

Conductivity measurements were made in a two-point probe configuration. The extremely high sample resistance made four-point probe measurements unnecessary since the contact resistance was negligible compared to the sample resistance. All contacts were verified to be Ohmic prior to use.

All anneals were performed in a high-vacuum furnace with a base pressure of 4×10^{-6} Torr. All irradiations were performed with 600 keV Kr^{++} ions with total doses equal to or greater than one displacement per atom (dpa), as calculated using the TRIM^{18–20} collision cascade simulation program. A total dose of 1 dpa is known to be the saturation dose at which *a*-Si unrelaxes completely.¹⁰ The beam-spot size was approximately 1 cm^2 , and the beam was rastered across the sample in excess of 1 KHz.

For *in situ* conductivity measurements, samples were mounted either onto a resistively heated metal hot stage for elevated temperature measurements, or onto a liquid-cooled cold stage with heat conducting paste for low-temperature measurements. For high-temperature experiments, sample temperature was measured by a thermocouple clipped onto the sample surface. For the low-temperature experiments, the sample temperature was assumed to be equal to the stage temperature. Simultaneous measurement of ion-beam current, sample current, and sample temperature proved to be difficult. Thus, for *in situ* experiments, ion-beam current was measured indirectly by first stabilizing the beam at the desired dose rate, and then adjusting parameters so as to maintain a constant total accelerating current and sample secondary electron current. The accuracy of dosimetry measurements made in this fashion is calibrated by Rutherford backscattering spectroscopy (RBS) measurements to be within $\pm 15\%$. This level of accuracy in dosimetry is acceptable, since the total dose in each case greatly exceeded 1 dpa.

III. EXPERIMENTAL CONDUCTIVITY MEASUREMENTS

A. Temperature-dependent conductivity of relaxed amorphous silicon

The variation of conductivity with measurement temperature for amorphous silicon first relaxed by annealing at 873 K for 15 min is illustrated in Fig. 1. The values obtained are in good agreement with previous reports of conductivity of *a*-Si.¹¹ There is a clear change in the tem-

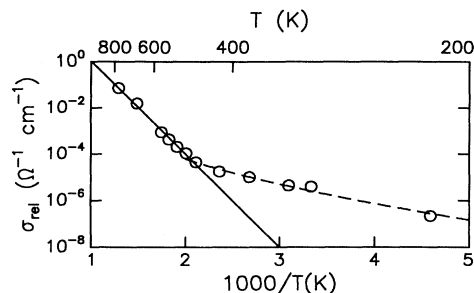


FIG. 1. Temperature dependence of conductivity of relaxed *a*-Si. Samples were relaxed by an 873 K anneal prior to measurement. The solid line is fit to $\sigma \propto \exp(-E/kT)$ behavior, and the dashed line is fit to $\sigma \propto \exp[-(B/T)^{1/4}]$ behavior. The fit yields $E = 0.8 \text{ eV}$, and $B = 110 \text{ K}^{1/4}$.

perature dependence of conductivity near 473 K. For measurement temperatures greater than 473 K, the conductivity shows $\exp(-1/T)$ dependence. The solid line is a least-squares fit to a functional form of $\sigma_{\text{rel}} = \sigma_0 \exp[-(E_c - E_f)/kT]$. The values obtained for σ_0 and $(E_c - E_f)$ are $1.1 \times 10^4 \text{ } \Omega^{-1} \text{ cm}^{-1}$ and 0.8 eV, respectively. For lower temperatures, more extensive observations of the temperature dependence of *a*-Si conductivity have indicated that conductivity depends as $\exp(-T^{-1/4})$ up to room temperature,²¹ which was the highest temperature used for the experiments. We note that previous work has indicated that *a*-Ge, which has a band gap of about 0.6 eV and activation energy for high-temperature conductivity of 0.25 eV, also shows $\exp(-T^{-1/4})$ behavior up to room temperature.²² Amorphous silicon has a band gap of about 1.4 eV and activation energy for high-temperature conductivity of 0.8 eV. Therefore, it is reasonable to assume that hopping conduction must dominate at much higher temperatures in *a*-Si than in *a*-Ge. Consequently, a functional form of $\sigma = \sigma_0^h \exp(-A/T^{1/4})$ was fitted, and is found to fit the data well. The values obtained for σ_0^h and A are $8.4 \times 10^5 \text{ } \Omega^{-1} \text{ cm}^{-1}$ and $110 \text{ K}^{1/4}$, respectively.

B. Variation of conductivity with anneal temperature

To discern the relationship between the extent of structural relaxation and conductivity, samples were first unrelaxed by irradiation at room temperature to a total dose of 1 dpa and then partially relaxed by annealing at various temperatures for 15 min. Conductivity of all samples was then measured at room temperature. Since samples were stored at room temperature, the value of conductivity after anneal at room temperature is taken to be that which is measured 15 min after termination of ion irradiation. For samples annealed at less than 473 K, Al contacts were applied prior to irradiation and post-irradiation annealing. For samples subject to anneal at higher temperatures, contact evaporation was the last step prior to the measurement of conductivity. Figure 2 illustrates the measured room-temperature conductivity. The solid curve is a guide to the eye. The values of con-

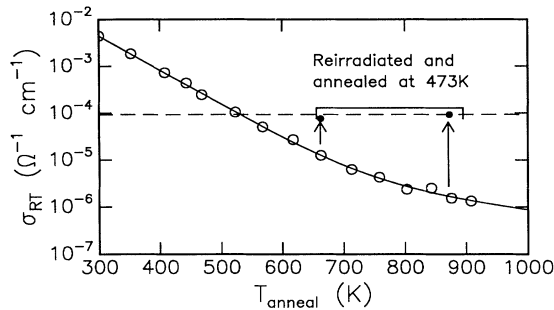


FIG. 2. Room-temperature conductivity of partially relaxed *a*-Si as a function of annealing temperature. All samples were unrelaxed prior to anneals. The solid circles are values of conductivity of samples initially annealed at indicated temperatures after reirradiation. The solid line is a guide to the eye. The dashed line is the value of conductivity of *a*-Si after initial relaxation by anneal at 473 K.

ductivity of two samples that were reirradiated to 1 dpa are also shown as solid circles. Contact evaporation again required a prebake at 473 K. As indicated by Fig. 2, post-anneal irradiation causes the conductivity to revert back to the value of the original sample annealed at 473 K, represented by the broken line.

C. *In situ* measurements of conductivity

Prior to *in situ* conductivity measurements, samples were first relaxed by annealing at 873 K for 15 min. Figure 3 shows *in situ* conductivity measurements made before, during, and after irradiation at various irradiation temperatures. Throughout the measurements, samples were held at the irradiation temperature. The dose rate was 7×10^{11} ions $\text{cm}^{-2} \text{sec}^{-1}$, and the irradiation time was 30 min. Thus the total dose is calculated to be approximately 3 dpa. The conductivity is normalized to the value prior to the start of irradiation. No data are given for the sample irradiated at 77 K because conductivity was unmeasurably small prior to irradiation. However, the observed changes in conductivity were similar in

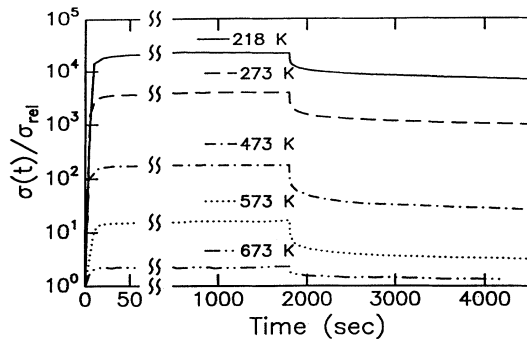


FIG. 3. *In situ* measurement of conductivity of initially relaxed *a*-Si during and after ion irradiation. The sharp drop in conductivity marks the end of irradiation. The conductivities are normalized to the initial value at the irradiation temperature. Notice the change in the scale of x axis.

behavior to those irradiated at higher temperatures. Note that the scale of the abscissa of Fig. 3 changes abruptly in order to show the extremely rapid increase in conductivity upon the onset of irradiation. All curves show a similar rapid and immediate increase in conductivity upon onset of irradiation, and quick saturation to an apparent steady-state value. It is apparent that lower implantation temperatures correspond to greater increases in conductivity. The rapid conductivity decay in Fig. 3 marks the moment when ion irradiation was terminated. The conductivity transient after termination of irradiation is extremely rapid at first, and but soon exhibits a slow decay, which continues even 45 min after the end of ion irradiation.

For the sample irradiated at 773 K, however, the measured change of conductivity is different from others, and is shown separately in Fig. 4. The conductivity rises rapidly, and saturates to an apparent steady-state value, as at other irradiation temperatures, but after ~ 10 min, it starts to increase rapidly and linearly with time. Irradiation of this sample was stopped earlier than other samples, but the total dose was still greater than 1 dpa. The decrease in conductivity following termination of irradiation is small, but measurable, and will be shown in more detail later in Fig. 5.

The most plausible explanation for the increase in conductivity during irradiation at 773 K after reaching an apparent steady-state value is the onset of crystal nucleation in *a*-Si. Since crystalline Si has much higher conductivity than *a*-Si, crystal, nucleation will irreversibly increase the sample conductivity. Ion irradiation is known to greatly enhance the rate of crystal nucleation in an *a*-Si matrix,²³ and the irradiation parameters were such that the onset of crystal nucleation is anticipated; indeed, presence of crystal grains was later confirmed by x-ray diffraction. Furthermore, the observed change in conductivity is consistent with crystallization exhibiting an incubation period followed by a steady-state nucleation at a constant rate.

Part of the fluctuation of conductivity both during and after irradiation, especially those observed for samples at high temperatures, is due to fluctuations in temperature, which could be maintained only to within $\pm 3^\circ\text{C}$ for elevated temperature measurements. Part of the fluctuation of conductivity during ion irradiation, however, was due to fluctuation in ion flux. Indeed, it was observed

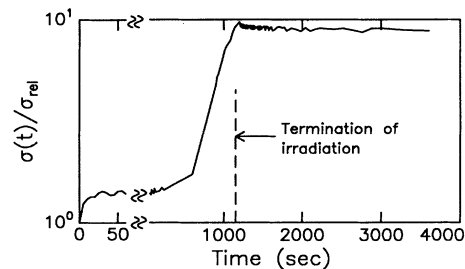


FIG. 4. *In situ* measurement of conductivity of initially relaxed *a*-Si irradiated at 773 K. The scatter in data after the termination irradiation is due to fluctuations in temperature. Notice the change in the scale of x axis.

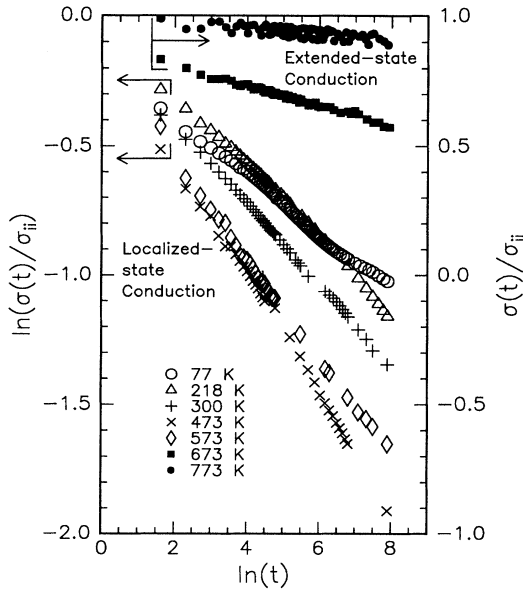


FIG. 5. Conductivity transients for *in situ* measurements, plotted against $\ln(t)$. Left vertical axis is the logarithm of conductivity normalized to the value of conductivity during irradiation. The right vertical axis is the value of conductivity normalized to the value during irradiation.

that conductivity increased when the ion flux increased. Finally, some samples were reannealed at 873 K for 15 min following irradiation, and the room-temperature conductivity of such samples were verified to revert to the preimplantation value.

IV. THEORY FOR RELATION OF ELECTRICAL CONDUCTIVITY TO DEFECT DYNAMICS

Before analyzing the data quantitatively, we will first discuss the aspects of the theories of structural relaxation of amorphous solids and of electrical conduction in amorphous semiconductors that are relevant to this paper. In doing so, we will follow the arguments given by Gibbs²⁴ and Mott,²⁵ for structural relaxation and conductivity, respectively.

A. Theory of activation-energy spectrum and relaxation in amorphous materials

The theory of activation-energy spectra and structural relaxation in amorphous materials was developed in the study of structural relaxation in metallic glasses, but is thought to be applicable to amorphous materials in general. In studies of metallic glasses, it was shown to be successful in describing reversible and irreversible property changes, and the “ $\ln(t)$ behavior” that characterizes many relaxation processes under isothermal anneal.²⁶

As treated by Narayanaswami,²⁷ and further developed by Gibbs, the main assumption of the activation-energy spectrum theory is that the activation energies of processes (i.e., any thermally activated transport or rearrangement of single atoms or groups of atoms) that contribute to structural relaxation are continuously distributed in

activation energy. This assumption naturally leads to the definition of $D(Q)$, the density of relaxation processes with activation energy Q . Hence, $D(Q)dQ$ is the number of relaxation processes that have activation energy between Q and $Q+dQ$. Strictly speaking, interaction between processes with different activation energies must be taken into account. However, in this theory, it is assumed that various relaxation processes are at least locally independent of each other; that is, activation of relaxation processes within an energy range between Q and $Q+dQ$ is assumed not to change the density of relaxation processes in other energy ranges.

The density of relaxation processes, $D(Q)$, however, cannot be measured directly, but it can be inferred by measuring a change of some property which changes as the material relaxes, such as the conductivity. We begin by writing the change due to relaxation as follows:

$$\Delta P = \int dp = \int p(Q)dQ = \int C(Q)D_i(Q)dQ, \quad (1)$$

where $p(Q)$ is the change in property being measured due to activation of relaxation processes with activation energy between Q and $Q+dQ$, $D_i(Q)$ is the density of relaxation processes that have contributed to relaxation at time t , and $C(Q)$ is the function that relates $p(Q)$ to $D_i(Q)$.

We can further define $\theta(Q, T, t)$, the characteristic annealing function, such that

$$D_i(Q)dQ = D(Q)\theta(Q, T, t)dQ. \quad (2)$$

The characteristic annealing function $\theta(Q, T, t)$ gives the proportion of the density of relaxation processes $D(Q)$ at energy Q that have contributed to relaxation as a function of annealing temperature T and annealing time t . The exact functional form of $\theta(Q, T, t)$ depends upon the order of reaction that leads to relaxation. If relaxation occurs through a first-order reaction, then

$$\theta(Q, T, t) = 1 - \exp \left[-\nu t \exp \left(\frac{-Q}{kT} \right) \right]. \quad (3)$$

If relaxation occurs through a second-order reaction,

$$\theta(Q, T, t) = 1 - \frac{1}{1 + \nu t \exp(-Q/kT)}. \quad (4)$$

For both Eqs. (3) and (4), the reaction constant ν is expected to be of the order of 10^{12} – 10^{14} sec^{-1} . The significance of $\theta(Q, T, t)$ lies not in its exact shape, but in its rapid change from 0.95 to 0.05 within a narrow range of activation energies, of the order of a few kT . Thus, if $D(Q)$ is broad and slowly varying, we can approximate $\theta(Q, T, t)$ with a step function at an energy $Q_\ominus = kT \ln(\nu t)$ such that

$$\begin{aligned} \theta(Q, T, t) &= 1, & Q < Q_\ominus, \\ \theta(Q, T, t) &= 0, & Q > Q_\ominus. \end{aligned} \quad (5)$$

For irradiation-induced defects in *a*-Si, there is considerable experimental evidence which suggests that relaxation occurs through a second-order reaction.^{2,10,28} The order of reaction is unimportant for the present analysis, however, since this approximation is valid for both first- and

second-order reaction kinetics. Indeed, the main conclusions of the theory of activation-energy spectrum do not depend sensitively on the order of reaction. This also implies, however, that we cannot distinguish between different orders of reaction using this method.

It is important to note that while Q_{\odot} depends linearly on anneal temperature, it depends only logarithmically on anneal time. Therefore, during an isothermal anneal of a typical experimental duration, Q_{\odot} will sweep only a narrow activation-energy range after a brief transient. If neither $D(Q)$ nor $C(Q)$ have sharp features of the order of the energy range swept by Q_{\odot} , we can greatly simplify Eq. (1) as follows:

$$\Delta P = \int^{Q_{\odot}} C(Q)D(Q)dQ = C_0 D_0 kT \ln(vt) \propto \ln(t), \quad (6)$$

where C_0 and D_0 are the average values of $C(Q)$ and $D(Q)$ within the energy range swept by Q_{\odot} during the anneal, respectively. Thus, a property of amorphous material will change logarithmically with time if there exists a density of activation energies for relaxation, and if the approximations used in deriving Eq. (6) are valid.

B. Electron transport in amorphous semiconductors

Optical and electrical measurements have shown the Mott²⁵ theory of electron conduction in amorphous solids to be successful in explaining the observed electrical properties of pure (i.e., unhydrogenated), undoped, and tetrahedrally bonded amorphous semiconductors, such as *a*-Ge or *a*-Si.²⁹⁻³¹ Within this theory, the concepts of electronic density of states $g(E)$ and band gap are considered to be still valid for amorphous materials. The lack of long-range order is thought to create a large density of localized states near the band edges, and electron mobilities in these localized band tail states are thought to be about three orders of magnitude smaller than the mobility in extended states. Furthermore, other defects inherent to amorphous solids are thought to create a band of localized states near the middle of the energy gap which pin the Fermi level. Conduction, then, is characterized by three different mechanisms, dependent upon the temperature. Conduction will occur through either (a) phonon-assisted tunneling ("hopping") of electrons near the Fermi level, or (b) hopping conduction of electrons in localized band tails, or (c) extended state (nonlocalized) conduction.

At sufficiently high temperatures, enough electrons are excited to extended states to dominate the conduction process. In this case, the conductivity is given by

$$\sigma_{\text{ext}} = \sigma_0^x \exp[-(E_c - E_F)/kT]. \quad (7)$$

At moderate temperatures, conductivity is thought to be dominated by localized state transport in the band tail states, and is treated in a way similar to extended state conduction, that is,

$$\sigma_{\text{tail}} = \sigma_0^t \exp[-(E_c - E_F + W)/kT], \quad (8)$$

where W is the activation energy for hopping. As is with σ_0^x, σ_0^t is difficult to estimate, but is expected to be at least three orders of magnitude less than σ_0^x , since the mobility

in localized states is smaller by this factor.

At low temperatures, conduction is expected to be dominated by hopping of electrons within the order of kT from the Fermi level, and is given by

$$\sigma_{\text{hop}} = \sigma_0^h \exp(-A/T^{1/4}). \quad (9)$$

This $\exp(-T^{-1/4})$ dependence of conductivity on temperature is widely accepted and observed for amorphous semiconductors. We note, however, that the specific form of σ_0^h and A remain controversial. Assuming that the electron mobility obeys Einstein's relation and approximating the density of electronic states near the Fermi level to be constant, Mott²⁵ derived the following:

$$\sigma_0^h = \frac{e^2}{10} \gamma \left[\frac{g(E_F)}{\alpha kT} \right]^{1/2} \quad (10)$$

and

$$A = 2.1 \left[\frac{\alpha^3}{g(E_F)k} \right]^{1/4}, \quad (11)$$

where e is the charge of an electron, γ is the attempt frequency of localized electrons, α^{-1} is the decay constant of localized electron wave functions, and $g(E_F)$ is the density of electronic states at the Fermi level. It must be noted, however, that deviations from the simplifying assumptions used in obtaining Eqs. (10) and (11) will lead to slightly different results. We will assume Eqs. (10) and (11) to be accurate; however, it will be shown in the following that for the most part, it is sufficient for the pre-factor σ_0^h to be only some weak function of $g(E_F)$, and for the exponential factor A to be proportional to $g(E_F)^n$, where n is an exponent near 1/4.

Both *in situ* and *ex situ* measurements suggest clearly that relaxation is associated with a decrease in conductivity. Furthermore, if we assume that α^{-1} , the decay constant for the electron wave function, is constant, then the measurements strongly suggest that $g(E_F)$, the density of electronic states near the Fermi level, is a function of the degree of relaxation of *a*-Si. Unrelaxation increases $g(E_F)$, and relaxation decreases it. Previous reports of the effect of ion irradiation on conductivity of *a*-Ge and *a*-Si are consistent with this interpretation.³²

Relaxation, however, is associated with annihilation of point defects, whose activation energies are believed to form a continuous spectrum.¹⁰ Since the localized electronic states near the Fermi level are presumed to have been created by defects, we define a function $G(Q)$, the density of relaxation states with activation energy Q associated with localized electron states near the Fermi level, such that

$$g(E_F) = \int G(Q)dQ. \quad (12)$$

Since we are assuming that defects which affect $g(E_F)$ are representative of all defects [including those without any effect on $g(E_F)$] we further assume that $G(Q)$ is proportional to $D(Q)$, the overall spectrum of activated processes for relaxation of *a*-Si.

Information about the existence and qualitative features of $G(Q)$ can be obtained from the *in situ* mea-

surement of conductivity. It is important to note that as samples are being irradiated, they also undergo an unavoidable thermal anneal at the irradiation temperature T_{ii} , and for the irradiation time t_{ii} ; thus the post-irradiation anneal is essentially a continuation of the anneal. At the end of irradiation, therefore, most of the defect states in $G(Q)$ with activation energies below $Q' \approx kT_{ii} \ln(\nu t_{ii})$ will have already contributed to relaxation, while only a few of the defect states in $G(Q)$ above $Q' \approx kT_{ii} \ln(\nu t_{ii})$ will have contributed to relaxation. Changes in conductivity (after a short transient to ensure that both the excess carries generated by irradiation and the defects with low activation energies created just prior to termination of irradiation have all recombined) measured after termination of irradiation will then reflect the decrease in $g(E_F)$. Since Q_\odot depends logarithmically on total anneal time, Q_\odot will increase only very slightly during the 45 min anneal; correspondingly, $g(E_F)$ will decrease only slightly, such that $\Delta g/g$ is small at all times.

In such cases, we can isolate the changes in $g(E_F)$. Letting $g'(E_F) = g(E_F) - \Delta g(E_F)$, we can combine Eqs. (9) and (11) to obtain

$$\frac{\sigma'}{\sigma} = \frac{\sigma(g')}{\sigma(g)} = \frac{\sigma_0^h(g')}{\sigma_0^h(g)} \exp \left\{ -2.1 \left[\frac{\alpha^3}{gkT} \right]^{1/4} \times \left[\left[\frac{g}{g'} \right]^{1/4} - 1 \right] \right\}. \quad (13)$$

Expanding $(g/g')^{1/4}$, and neglecting higher-order terms,

$$\frac{\sigma'}{\sigma} = \frac{\sigma_0^h(g')}{\sigma_0^h(g)} \exp \left[-\frac{2.1}{4} \left[\frac{\alpha^3}{gkT} \right]^{1/4} \frac{\Delta g}{g} \right]. \quad (14)$$

If the prefactor σ_0^h is some weak function of $g(E_F)$, then we can neglect it in comparison with the exponential when taking the logarithm of both sides. In such cases, we have

$$\ln \left[\frac{\sigma'}{\sigma} \right] = -\frac{2.1}{4} \left[\frac{\alpha^3}{gkT} \right]^{1/4} \frac{\Delta g}{g}. \quad (15)$$

Therefore, in the cases where hopping conduction is appropriate, the logarithm of the normalized conductivity will be proportional to the changes in the density of electronic states near the Fermi level $g(E_F)$. Now the assumptions made in deriving Eq. (6), which predicted a $\ln(t)$ behavior, hold. If there indeed exists a $G(Q)$, and if it is broad and slowly varying, then we expect the logarithm of normalized conductivity to decrease as $\ln(t)$.

Figure 5 illustrates the measured decay of conductivity starting 5 sec after termination of irradiation, plotted against $\ln(t)$. For low temperatures where we expect hopping conduction to be the dominant conduction mechanism, $\ln(\sigma'/\sigma)$ is plotted; for high temperatures where we expect the extended state conduction to be the dominant conduction mechanism, (σ'/σ) is plotted instead. Hopping conduction was assumed to be the dominant carrier transport mechanism for the sample irradi-

ated at 573 K because previous reports have suggested that unrelaxation tends to increase the temperature at which transition from hopping conduction to extended state conduction occurs.¹¹ Indeed the conductivity decrease after termination of irradiation at 573 K more closely resembles the one at 473 K than the one at 673 K; thus it is deemed appropriate to assume hopping conduction at 573 K. Most curves display excellent linearity, and the rates of decay for the low-temperature relaxation (≤ 573 K) are all similar. The two measurements made at low temperatures deviate somewhat from linear behavior, but can still be approximated by a straight line.

The observed " $\ln(t)$ " decay of conductivity for low temperatures (≤ 573 K) indicates clearly that the density of electronic states near the Fermi level $g(E_F)$ is decreasing as $\ln(t)$, which in turn indicates that there indeed exists $G(Q)$, the density of activation states with activation energy Q associated with localized electron states near the Fermi level. Furthermore, the " $\ln(t)$ " behavior also indicates that $G(Q)$ is a slowly varying function that is nearly constant on a scale of a few tenths of an electron volt which is the energy range spanned by the postirradiation anneal. The fact that the two samples, irradiated and annealed, below room temperature deviate somewhat from the linear decay might be an indication of some features in activation-energy spectrum at low activation energies. However, the fact that they can be approximated by a straight line means that $G(Q)$, and also presumably $D(Q)$, the total density of relaxation states with activation energy Q , also have nonzero values in the low- Q range, in this case below 0.23 eV. The high-temperature (≥ 573 K) data suggest that $G(Q)$ probably extends into high activation-energy ranges as well, although in such cases Eq. (15) is clearly invalid, since conduction at these high temperatures is dominated by extended state conduction. It is possible that the onset of crystal nucleation has rendered the sample irradiated at 773 K a composite of amorphous and crystalline silicon whose conductivity is not amenable to simple interpretation. Nonetheless, the fact that conductivity does decrease is evidence that some relaxation does occur in the *a*-Si even when irradiated at high temperatures, and that $G(Q)$ probably extends into high activation-energy ranges.

V. ACTIVATION-ENERGY SPECTRUM

A more quantitative insight into $G(Q)$ is possible from changes in room-temperature conductivity following 15 min isochronal anneals at different temperatures. We rewrite Eq. (12) as follows:

$$g(E_F) = g_0 + \int_{Q_\odot(T)}^{Q_\odot^0} G(Q) dQ, \quad (16)$$

where g_0 is the electronic density of states at the Fermi level after 873 K anneal. The upper limit of integration is the value of Q_\odot after 873 K anneal, and the lower limit is $Q_\odot(T)$ after anneal at temperature T . Now we rewrite Eq. (13) as follows:

$$\frac{\sigma'}{\sigma} = \frac{\sigma_0^h(g')}{\sigma_0^h(g_0)} \exp \left\{ -2.1 \left[\frac{\alpha^3}{g_0 kT} \right]^{1/4} \times \left[\left[\frac{g_0}{g_0 + \int G(Q)dQ} \right]^{1/4} - 1 \right] \right\}. \quad (17)$$

From Fig. 1, we know the value of the factor $2.1(\alpha^3/g_0 kT)^{1/4}$ to be 26.43 at room temperature. If we assume a reasonable value for α^{-1} , we can also calculate the value for g_0 , assuming α^{-1} to be $\approx 10 \text{ \AA}$, we find that $g_0 \approx 1.45 \times 10^{18} \text{ eV}^{-1} \text{ cm}^{-3}$. Taking the logarithm of both sides of Eq. (17), and again neglecting the prefactor in comparison with the exponent, we can isolate $G(Q)$:

$$G(Q') = -\frac{d}{dQ'} \int_{Q_0(T)}^{Q_0^0} G(Q)dQ = -g_0 \frac{d}{dQ'} \left[1 - 0.038 \ln \left[\frac{\sigma'}{\sigma_0} \right] \right]^{-4}. \quad (18)$$

In order to perform this differentiation, it is necessary to convert the abscissa of Fig. 2 from anneal temperature to activation energy Q . This requires an estimate of the reaction constant ν . We assume ν to be of the order of the Debye frequency, or 10^{13} sec^{-1} for silicon. Similar values have been used previously for recombination of ion-induced defects.^{10,28} The result of differentiation, using 10^{13} sec^{-1} for ν , is illustrated in Fig. 6. As expected, $G(Q)$ is broad, and extends from 0.9 eV to greater than 2.7 eV. It also seems to extend to lower values of activation energy Q , corroborating the results of *in situ* measurements made below room temperature. It must be pointed out, however, that the energy range probed by below-room-temperature irradiation or anneal lies outside the region covered by the deduced activation-energy spectrum in Fig. 6, and thus no quantitative conclusion can be drawn about activation-energy spectrum at low ($\leq 0.9 \text{ eV}$) activation energies. The activation-energy spectrum decreases slowly and monotonically with increasing activation energy with no sharp features, thus

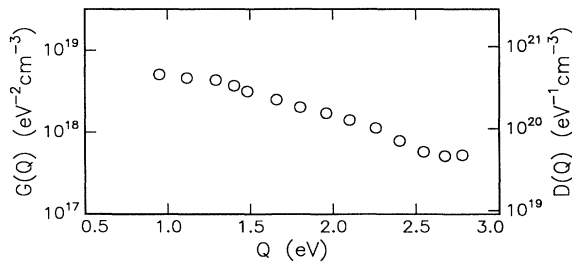


FIG. 6. Density of electronic states near the Fermi level $G(Q)$, associated with relaxation activation energy Q , as derived from Fig. 3. The right-hand ordinate indicates the activation-energy spectrum $D(Q)$ inferred from the density of electronic states.

justifying approximations that we employed in deriving it. This shape is consistent with results by Roorda *et al.*¹⁰ who have found that heat released during relaxation decreases with increasing temperature. Lack of any discernible features in the activation-energy spectrum does not contradict *in situ* low-temperature measurements (which indicated the possibility of some features), since the range of activation energies covered in Fig. 6 does not extend to such low values. Furthermore, although not shown, the qualitative shape of $G(Q)$ was confirmed to be relatively insensitive to the exponent of $g(E_F)$.

As mentioned before, electrically active defects are assumed to be representative of all defects in *a*-Si responsible for structural relaxation. The activation-energy spectrum for overall structural relaxation of *a*-Si, $D(Q)$, may be estimated by comparing the saturation value of g with the estimated density of defects for fully unrelaxed *a*-Si, which is found to be of the order of 1 at. % *a*-Si.^{10,14} Only electrons within order of kT from the Fermi level dominate the conduction process. We can therefore neglect the possibility of multiple electronic levels per defect. Assuming that one defect creates one electronic state, we find $D(Q) \approx 90 \text{ eV} G(Q)$. The estimated value of $D(Q)$ is given on the right vertical axis of Fig. 6.

Care must be taken in interpreting Fig. 6, since rigorous conversion of annealing temperature to activation energy requires knowledge of the reaction constant ν . But because Q_0 depends only logarithmically on ν , the conversion is fairly insensitive to errors in estimation. Indeed, $\Delta\nu$ would have to be greater than one order of magnitude for there to be a significant shift in the activation-energy scale. It is still interesting to note that $G(Q)$ seems to reach negligible values at activation energies greater than 2.8 eV. So far, experimental investigation of relaxation processes with activation energies beyond the upper limit of 2.6 eV have not been probed thoroughly due to the intervention of crystallization. Raman spectroscopy has indicated that structural relaxation of *a*-Si continues up to 1123 K,³³ but the annealing times for the higher temperature ($\geq 1073 \text{ K}$) anneals were much shorter than the annealing times for lower temperature anneals. The maximum activation energy probed in that work was 2.5 eV, and it is not clear whether this experiment probed states more relaxed than can be achieved via a 15 min anneal at 903 K, or whether the relaxation process was simply accelerated. On the other hand, the relative dearth of relaxation processes with activation energies greater than 2.8 eV is tantalizing, since 2.7 eV is the activation energy of the rate of solid-phase epitaxy (SPE) of crystalline Si into *a*-Si. Unlike any processes involving *a*-Si, the rate of SPE has been shown to be conspicuously independent of the degree of relaxation,³⁴ and is characterized by a single activation energy ($Q = 2.7 \text{ eV}$) over nearly ten orders of magnitude in the solid-phase epitaxy rate.³⁵ Such a dearth of relaxation processes with activation energies greater than 2.7 eV is consistent with the notion that structural relaxation and solid-phase epitaxy are controlled by different processes. Structural relaxation is by nature a bulk phenomenon, whereas there is strong evidence that solid-phase epitaxy

is limited by interface rearrangement kinetics.³³ Furthermore, the likeliest candidate for the controlling event in solid-phase epitaxy is dangling bond rearrangement,^{34,36} while recent reports suggest that structural relaxation is associated with annihilation of vacancylike defects in *a*-Si.^{37–39}

One other remarkable consequence of this analysis, as evidenced by presence of defects with high activation energies and the *in situ* measurement of relaxation at high temperature, is the ability of irradiation to maintain an excess concentration of structural defects in *a*-Si during irradiation even when the sample temperature during irradiation is high (573–773 K). In other words, irradiation creates a substantial number of defects with relatively high activation energies and long lifetimes to measurably increase the steady-state defect concentration during irradiation at 773 K relative to the defect concentration following a 773 K anneal. Such increased defect concentration has been demonstrated to substantially increase the defect enthalpy and thus the overall free energy of *a*-Si.¹⁰ The absolute increase in defect enthalpy is anticipated to be small for irradiation temperatures greater than 673 K. Nonetheless, we proposed earlier that such transient unrelaxation of *a*-Si under irradiation might be an explanation for the observed anomalous enhancement of the crystal nucleation rate in an amorphous silicon matrix, since the nucleation rate is extremely sensitive to small changes in free energy⁴⁰ (e.g., even a 10% increase in driving force can conceivably result in a five to seven order of magnitude increase in nucleation rate). Recently, we have also shown experimentally that irradiation-induced changes in the thermodynamic driving force for crystallization cannot be neglected in irradiation-enhanced nucleation.⁴¹ The present results are more direct evidence that an irradiation-induced increase in defect enthalpy is an important component in driving force for beam-induced crystallization at higher temperatures.

VI. CONCLUSION

Through measurement of irradiation-induced conductivity changes, we have probed $G(Q)$, the density of relaxation states associated with localized electron states near the Fermi level. It is a slowly decreasing function extending from below 1.0 eV to beyond 2.6 eV, and probably extending to below 0.23 eV. The dearth of defect states with activation energy greater than the activation energy for solid-phase epitaxy is consistent with the notion that structural relaxation and solid-phase epitaxy are controlled by different processes, and may explain the observed independence of the rate of solid-phase epitaxy from the extent of structural relaxation. *In situ* measurements of conductivity show that $G(Q)$ decreases linearly with $\ln(t)$ following irradiation, consistent with the predictions of an activation-energy spectrum model and further supporting the conclusion that $G(Q)$ varies slowly over the energy range investigated. High-temperature irradiation shows that even at elevated irradiation temperatures (≤ 773 K), ion irradiation unrelaxes *a*-Si, and that under ion irradiation, the steady-state defect concentration is maintained at a level higher than that following post-irradiation annealing. This observation supports a model for ion-irradiation-enhanced nucleation which asserts that excess defect enthalpy in *a*-Si leads to an increase in the free energy of *a*-Si relative to *c*-Si, thus increasing the driving force for crystal nucleation.

ACKNOWLEDGMENTS

We thank J. Reid for depositing the Ti/N/Si diffusion barrier and silver contacts, and for insight on contact metallization, and Dr. J. S. Im for helpful discussions. We also would like to thank Kyoung-Hee Kim for performing the x-ray analysis of partially crystallized samples. This work was supported by U.S. Department of Energy, Basic Energy Sciences, under Contract No. DE-FG-03-89ER45395.

¹C. N. Waddell, W. G. Spitzer, J. E. Frederickson, G. K. Hubler, and T. A. Kennedy, *J. Appl. Phys.* **55**, 4361 (1984).

²A. Witvrouw and F. Spaepen, in *Kinetics of Phase Transformations*, edited by M. M. Thompson, M. J. Aziz, and G. B. Stephenson, MRS Symposia Proceedings No. 205 (Materials Research Society, Pittsburgh, 1991), p. 21.

³S. Roorda, S. Doorn, W. C. Sinke, P. M. L. O. Scholte, and E. van Loenen, *Phys. Rev. Lett.* **62**, 1880 (1989).

⁴E. P. Donovan, F. Spaepen, J. M. Poate, and D. C. Jacobson, *Appl. Phys. Lett.* **55**, 1516 (1989).

⁵J. S. Lannin, L. J. Piloni, S. T. Kshirsagar, R. Messier, and R. C. Ross, *Phys. Rev. B* **26**, 3506 (1982).

⁶W. C. Sinke, T. Warabisako, M. Miyao, T. Tokuyama, S. Roorda, and F. W. Saris, *J. Non-Cryst. Solids*, **99**, 308 (1988).

⁷B. Park, F. Spaepen, J. M. Poate, and D. C. Jacobson, *J. Appl. Phys.* **69**, 6430 (1991).

⁸A. Polman, D. C. Jacobson, S. Coffa, J. M. Poate, S. Roorda, and W. C. Sinke, *Appl. Phys. Lett.* **57**, 1230 (1990).

⁹C. A. Volkert, *J. Appl. Phys.* **70**, 3521 (1991).

¹⁰S. Roorda, W. C. Sinke, J. M. Poate, D. C. Jacobson, S. Dirker, B. S. Dennis, D. J. Eaglesham, F. Spaepen, and P. Fuoss, *Phys. Rev. B* **44**, 3702 (1991).

¹¹W. Beyer and J. Stuke, in *Amorphous and Liquid Semiconduc-*

tors, Proceedings of the Fifth International Conference on Amorphous and Liquid Semiconductors, edited by J. Stuke and W. Brenig (Taylor & Francis, London, 1974), p. 251.

¹²Jung H. Shin, J. S. Im, and Harry A. Atwater, in *Phase Formation and Modification by Beam-Solid Interactions*, edited by Gary S. Was, David M. Follstaedt, and Lynn E. Rehn, MRS Symposia Proceedings No. 235 (Materials Research Society, Pittsburgh, 1992), p. 21.

¹³K. F. Kelton and F. Spaepen, *Phys. Rev. B* **30**, 5516 (1984).

¹⁴S. Coffa and J. M. Poate, *Appl. Phys. Lett.* **59**, 2296 (1991).

¹⁵M. H. Brodsky, in *Amorphous Semiconductors*, edited by M. H. Brodsky, 2nd ed. (Springer-Verlag, New York, 1985), p. 3.

¹⁶J. C. Bean and J. M. Poate, *Appl. Phys. Lett.* **36**, 59 (1980).

¹⁷J. R. Reid, E. Kolawa, T. A. Stephens, J. S. Chen, and M-A. Nicolet, in *Advanced Metallization for ULSI Applications*, edited by V. V. S. Rana, R. V. Joshi, and I. Ohdomari (Materials Research Society, Pittsburgh, 1992), pp. 285–291.

¹⁸J. F. Ziegler, J. P. Biersack, and U. Littmark, *The Stopping and Range of Ions in Solids* (Pergamon, New York, 1985).

¹⁹J. P. Biersack and L. J. Haggmark, *Nucl. Instrum. Methods* **174**, 257 (1980).

²⁰Copyright J. F. Ziegler, 1990.

²¹J. J. Hauser, *Phys. Rev. B* **8**, 3817 (1973).

- ²²M. L. Knotek and T. M. Donovan, *Phys. Rev. Lett.* **30**, 652 (1972).
- ²³J. S. Im and Harry A. Atwater, *Appl. Phys. Lett.* **57**, 1766 (1990).
- ²⁴M. R. J. Gibbs, J. E. Evetts, and T. A. Leake, *J. Mater. Sci.* **18**, 278 (1983).
- ²⁵N. F. Mott and E. A. Davis, *Electronic Processes in Non-Crystalline Materials* (Clarendon, Oxford, 1971), p. 42.
- ²⁶A. L. Greer, in *Rapidly Solidified Alloys: Processes, Structures and Properties*, edited by H. H. Liebermann (Marcel Dekker, New York, in press), Chap. 10.
- ²⁷O. S. Narayanaswamy, *J. Am. Ceram. Soc.* **61** 146 (1978).
- ²⁸K. A. Jackson, *J. Mater. Res.* **3**, 1218 (1988).
- ²⁹M. Pollak, M. L. Knotek, H. Kurtzman, and H. Glick, *Phys. Rev. Lett.* **30**, 856 (1973).
- ³⁰M. L. Knotek, M. Pollak, and T. M. Donovan, *Phys. Rev. Lett.* **30**, 853 (1973).
- ³¹P. Nagels, in *Amorphous Semiconductors* (Ref. 15), p. 113.
- ³²N. Apsley, E. A. Davis, A. P. Troup, and A. D. Yoffe, in *Amorphous and Liquid Semiconductors: Proceedings of the Seventh International Conference on Amorphous and Liquid Semiconductors*, edited by W. E. Spear (University of Edinburgh, Edinburgh, 1977) p. 447.
- ³³L. de Wit, S. Roorda, W. C. Sinke, F. W. Saris, A. J. M. Berntsen, and W. F. van der Weg, in *Kinetics of Phase Transformations*, edited by M. M. Thompson, M. J. Aziz, and G. B. Stephenson, MRS Symposia Proceedings No. 205 (Materials Research Society, Pittsburgh, 1991), p. 3.
- ³⁴G.-Q. Lu, Eric Nygren, and M. Aziz, *J. Appl. Phys.* **70**, 5323 (1991).
- ³⁵G. L. Olson and J. A. Roth, *Mater. Sci. Reports* **3**, 1 (1988).
- ³⁶J. A. Roth, G. L. Olson, D. C. Jacobson, and J. M. Poate, *Appl. Phys. Lett.* **57**, 1340 (1990).
- ³⁷S. Roorda, R. A. Hakvoort, A. van Veen, P. A. Stolk, and F. W. Saris, in *Phase Formation and Modification by Beam-Solid Interactions* (Ref. 12), p. 39.
- ³⁸P. A. Stolk, L. Calcagnile, S. Roorda, H. B. van Lindaen Van den Heuvel, and F. W. Saris, in *Phase Formation and Modification by Beam-Solid Interactions* (Ref. 12), p. 15.
- ³⁹G. N. Vandehoven, Z. N. Liang, L. Niesen, and J. S. Custer, *Phys. Rev. Lett.* **68**, 3714 (1992).
- ⁴⁰J. S. Im and H. A. Atwater, *Nucl. Instrum. Methods B* **59**, 422 (1991).
- ⁴¹Jung H. Shin and H. A. Atwater, *Nucl. Instrum. Methods B* (to be published).